

T. Palanisamy Sathishkumar\*, Shanmugam Arun Kumar, Palanisamy Navaneethakrishnan, Irulappasamy Siva and Nagarajan Rajini

# Synergy of cashew nut shell filler on tribological behaviors of natural-fiber-reinforced epoxy composite

DOI 10.1515/secm-2016-0243

Received August 16, 2016; accepted March 26, 2017; previously published online May 11, 2017

**Abstract:** The aim of this work is to investigate the adhesive dry sliding wear and friction performance of biodegradable cashew nut shell (CNS)-filler-reinforced epoxy composite. The composites are prepared with 5, 10, 15, 20, 25, 30, 35, and 40 weight content of CNS filler. Experiments were conducted to perform the required measurements. The results show that the specific wear rates and frictional coefficients are found lower at 30% untreated and treated CNS-containing composites. The NaOH-treated CNS filler composites showed low wear and frictional performance compared to raw CNS. The back film formation was associated with the predominant wear mechanics with the formation of fine debris on the worn surface and counterface.

**Keywords:** biodegradable materials; natural filler; polymer composite; wear.

## 1 Introduction

Owing to the rapid increase in competition in industrial markets, monitoring the development of innovative material designs for replacement is imperative. Accordingly, fiber-reinforced composite is identified as a well-known alternative with its less weight and higher stiffness, with economic advantage. Moreover, the recent issues on ecological friendliness to the society play a critical role in the consideration of addressing the regulations and policies

of the government related to material usage. Perhaps, it may be one of the reasons for the rapid implementation of natural-fiber-reinforced composites in many technological applications. Accordingly, tribology is one of the industrial sectors needed in the development of new materials toward energy conservation and minimization of material loss. Recently, lightweight, biodegradable, and user-friendly materials have been prepared by using natural fibers and fillers that are used as reinforcement for polymer to make natural-fiber-reinforced polymer composites and to study tribological behavior [1].

Natural fibers such as sisal, kenaf, snake grass, sugarcane, betelnut, bamboo, hemp, oil palm, and coir fibers have been used as reinforcement with various kinds of thermoplastic and thermoset matrices. This is due to their inexpensive nature and abundant availability resulting from the fast growth of the natural plant, better adhesion with matrix, processing in low cost, being light in weight, and being biodegradable and recyclable. All these are leading to a reduction in the dependency on petroleum sources. The usage of natural fibers in polymer composites is extensive today in many applications like roofing sheets, helmet, post box, laminates and panels for door frames, glove box, door panels, seat coverings, seat surface and backrest, trunk panel, trunk floor, and multipurpose tables [2]. Moreover, the use of natural-fiber-reinforced polymer composites needs considerable care, considering its extensive acceptance and commercial feasible. The wear and friction performance of specific natural-fiber-reinforced composites have been studied and are subjected to adhesive and abrasive wear condition.

Many authors have reported on the wear and friction performance of different natural fibers with polymer matrices. Bamboo fiber was extracted from the bamboo clumps of strips and chopped into required lengths to prepare epoxy composites. The wear resistance of the antiparallel orientation of the bamboo fiber composite was found to be better compared to that of the random and parallel orientations. At low sliding velocity, the friction performance showed a 44% improvement compared to the results obtained from the higher sliding velocity. A superior wear, friction, and

\*Corresponding author: T. Palanisamy Sathishkumar, Department of Mechanical Engineering, Kongu Engineering College, Erode, Tamilnadu, India, e-mail: tpsathish@kongu.ac.in; tpsathish81@gmail.com

**Shanmugam Arun Kumar:** Department of Mechanical Engineering, Velalar College of Engineering & Technology, Tamilnadu, India

**Palanisamy Navaneethakrishnan:** Department of Mechanical Engineering, Kongu Engineering College, Erode, Tamilnadu, India

**Irulappasamy Siva and Nagarajan Rajini:** Department of Mechanical Engineering, Kalasalingam University, Tamilnadu, India

temperature performance was seen with a counterface sliding velocity of 2.22 m/s [3].

Unidirectional sugarcane-fiber-reinforced polyester composites have higher wear resistance, twice as compared to chopped untreated sugarcane fiber polyester composites. This higher resistance demonstrated by the long fibers was well embedded in the matrix. The abrasive failure occurred at the end of the fibers, requiring high frictional energy to avoid failure. The sugarcane fiber length of 5 mm in polyester composites has better wear resistance compared to 1-mm and 10-mm fiber length [4]. The abrasive properties of random and unidirectional oriented sugarcane-fiber-reinforced polymer composites were significantly affected by the normal load. An increase in the normal load was followed by a wear loss of the composites in sliding velocity. The fiber length of 10 mm provided better wear performance compared to the composites with 1- and 5-mm fiber length. Also, the tangential abrasive force was high in long sugarcane fiber in polymer composites. This offered high wear resistance with better adhesion between the fiber and the matrix [5]; there was an increase in wear rate with increasing sugarcane fiber length, and the critical fiber length of 5 mm was found as the result of minimum wear rate [6]. Bagasse ash is obtained from the waste part of sugarcane. The ash was reinforced with recycled low-density polyethylene (RLDPE). The incorporation of ash in the RLDPE improved the wear resistance under dry wear testing compared to pure RLDPE. The wear rate was found to be low at 30% of ash in the RLDPE [7].

The applied load and sliding velocity play a significant role in wear performance. Enhanced wear resistance was obtained in normal orientation of kenaf fiber in the epoxy composites compared to parallel and antiparallel orientations. The friction coefficient was low in the antiparallel orientation at all load levels [8].

The wear rate was found to be low in dry conditions compared to wet conditions in the test of betel-nut-fiber-reinforced polyester composite. The presence of water (wet condition) in the composite enhanced the friction coefficients for all normal loads due to higher fiber pullout in the sliding surface [9]. The wear rate of treated betel-nut-fiber-reinforced epoxy composites was found to be low with the addition of abrasive sand particles of fine size. A similar trend was exhibited in the weight loss of the composites. The maximum wear rate was observed at a sliding velocity of 0.077 m/s [10].

The weight loss of chopped sisal-fiber-reinforced polypropylene composites increased with sliding distance. The 1% maleic anhydride grafted polypropylene (MA-g-PP) modified sisal-fiber-reinforced composite showed lower weight loss compared to untreated sisal fiber with

varying normal loads and sliding distances. The MA-g-PP coupling with an acid anhydride group agent formed a chemical bond with the hydroxyl groups of the lingo-cellulosic. This reduced the wear out of the specimen, which results in low wear rate [11].

The specific wear rate was low in unidirectional jute-fiber-reinforced polyester composites at TT sliding direction with an applied normal load of 60 N. The coefficient of friction was low in LT sliding direction at a normal load of 20 N [12]. The MA-g-PP melt-mixed jute-fiber-reinforced polypropylene composites were found to have a low volume of wear and wear rate compared to untreated jute-fiber-reinforced composites. This was the result of better adhesion between the fiber and matrix with the addition of MA-g-PP coupling agent on the fiber surface [13]. Jute fiber was treated with various chemicals such as alkali, permanganate, peroxide, silane 1, and silane 2 for preparing polylactide composites. The weight loss was found to be low in silane-2-treated jute polylactide composites for all sliding distances. Silane-2-treated fiber composite was found to have excellent wear behavior. This was observed by the shallow ploughed grooves or tiny scratches in the wear image, exhibiting the maximum abrasive wear resistance [14]. The wear performance of nettle-, *grewia-optiva*-, and sisal-fiber-reinforced polylactic acid (PLA) composites was improved by the addition of fiber in the composites. The coefficient of friction was low in *grewia optiva* fiber PLA composites compared to the other two [15].

Natural-fiber-reinforced polymer composites have found extensive applications in wear and frictional environments. The agricultural waste of palm fronds and mango dry leaf fillers was reinforced with polyester to make hard and fine filler-reinforced polyester composites. The dry mango leaves fiber polyester composites have low friction coefficient and high wear resistance. This is suitable for industrial applications like solid lubricants [16]. Hemp fiber is a reinforced material used for making non-asbestos organic brake materials. It consists of copper, antimony, trisulfide, phenolic resin, geopolymer, Kevlar fiber, abrasive, and organizes materials. Three different brake material samples were fabricated. Better wear results were obtained in a sample with 1.7% of hemp fiber, 0% of copper, and antimony trisulfide [17]. Jute fiber and powdered hazelnut shell were used for making non-asbestos, organic nonmetallic friction composites with additional materials such as wollastonite, basalt fibers, zircon, vermiculite, and binder of phenolic resin. A circular shape composite specimen was fixed in the chase tester. The 23.6% and 6.3% volume fractions of jute fibers and powdered hazelnut shells produced satisfactory tribological results. They showed the friction coefficient that was an

acceptable range for braking application [18]. The brake pad was fabricated by using ingredients such as graphite of 10% weight content (wt); 33% wt of aramid, lapinus, glass, steel, and brass; and 17% wt of friction modifiers such as alumina, vermiculite, and cashew dust with 30% wt of inert filler. The effect of pressure and velocity on the friction coefficients was discussed [19].

The above survey shows clearly the natural fibers as alternate materials for preparing composite friction materials with suitable binders. They need to achieve improvement in the friction material performance by treating the fiber with various chemicals prior to composite processing, considering that there is need for more work on the use of natural filler in friction material preparation and characterization. Only a limited number of works has been done on tribological application by using natural fibers and filler in the polymer composites for tribological study. No in-depth study has been made of the tribological behaviors of cashew nut shell (CNS) filler in polymer composites. It is a good natural filler material derived from the waste part in the cashew nut extraction process. It is a biodegradable material, and recently, CNS oil has been used as a resin (binder) to make friction materials.

The present work's aims are to prepare a biodegradable friction composite material and analyze the adhesive

wear and friction performance of CNS filler epoxy composites using a pin-on-disc (POD) machine under dry sliding condition. The different weight contents of CNS filler are considered in the preparation of the frictional composite materials. The worn-out surface morphology was examined by using a metallurgical microscope and scanning electron microscope (SEM). Dry sliding adhesive wear tests were conducted to analyze the wear rates and friction coefficients for various weight contents.

## 2 Materials

### 2.1 Preparation of CNS filler

Adult cashew nut fruits were plucked from cashew plants. A schematic representation of a cashew fruit is shown in Figure 1A. It consists of cashew (i.e. cashew apple) and seeds that consist of nut shell, testa, and kernel. The cashew seeds were removed from the cashew fruit and dried in sunlight for 3–4 days. Each seed was cut into two pieces to remove the cashew nuts (Figure 1B). The kernel and testa were removed from the seed and the remaining CNS (Figure 1C). The shell is a waste part of the cashew

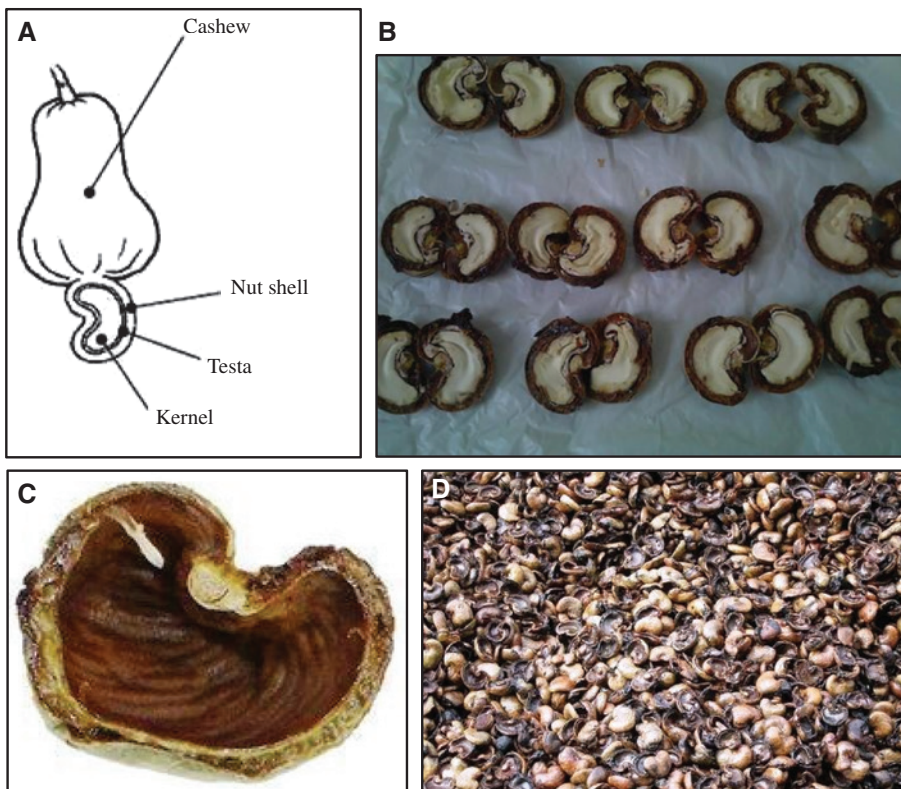


**Figure 1:** (A) Schematic representation of cashew fruit, (B) cashew nuts, (C) CNS and (d) drying process of CNSs.

seed and it is a biodegradable material. The waste shells were washed with plain water to remove the excess testa found inside the shells. The washed shells were dried in sunlight for 2 days to get them completely dry, as shown



Figure 2: CNS filler.

in Figure 1D. The dried shells were crushed in a ball mill to obtain the CNS fillers as a filler material of the composite (Figure 2). The filler dimension was maintained as 100  $\mu\text{m}$  to 50  $\mu\text{m}$  during crushing. The fillers were dried in sunlight for 48 h and post dried in an oven for an hour at 70°C [2] to obtain completely dry fillers.

## 2.2 Surface modification of CNS

CNS was immersed in a stainless-steel vessel containing 5% NaOH solution for half an hour [2]. During this process, the weak amorphous part in the fillers was removed to isolate the strong amorphous filler for the experiments. Again, these fillers were immersed in distilled water and washed thoroughly thrice to remove the excess acid present in the fillers. Final washing on CNS was done with water containing 1% acetic acid. Fillers were dried in normal atmospheric temperature for a day and in an air oven at 70°C for 3 h. Figure 3A and B shows the SEM of the raw and NaOH-treated CNS filler.

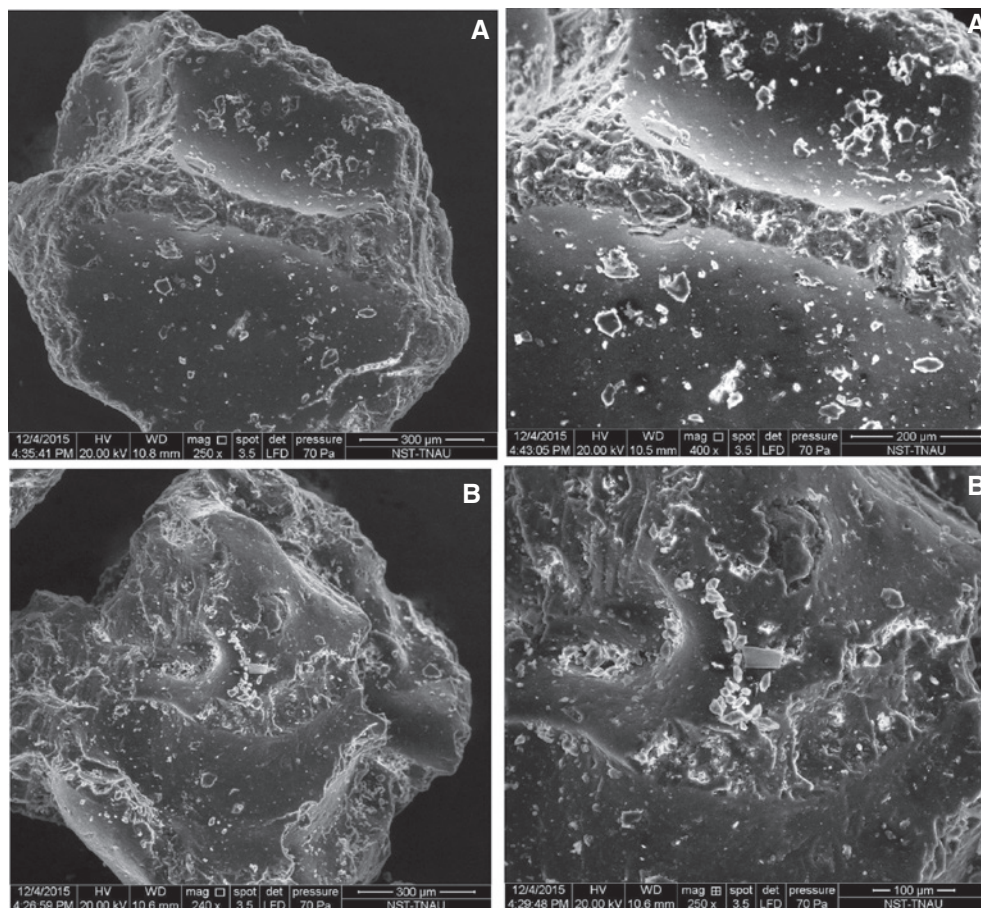


Figure 3: SEM image of CNS filler: (A) raw filler and (B) NaOH treated filler.

## 2.3 Mold

A steel mold setup was fabricated to prepare the composite specimen as shown in Figure 4A. It consists of three parts such as male (Figure 4Aa), female (Figure 4Ab), and supporting steel (Figure 4Ac) block. The total size of the male and female block was 120 mm (length)  $\times$  120 mm (width)  $\times$  12.5 mm (thickness). The female and male blocks have a projection on the surface with 2.5 mm thickness with a length of 100 mm and width of 100 mm. The dimension of the supporting block was 120 mm (length)  $\times$  120 mm (width)  $\times$  12.5 mm (thickness) with square hole of 100 mm (length)  $\times$  100 mm (width)  $\times$  12.5 mm (thickness). The supporting block was kept on the female block of 2.5 mm projection, and the male block of 2.5 mm projection was kept in the supporting block square hole. However, the gap between the female and male blocks was 10 mm with the supporting blocks, which is used to prepare the composite plate of 100 mm (length)  $\times$  100 mm (width)  $\times$  10 mm (thickness) size. The schematic diagram of the composite mold is shown in Figure 4B.

## 2.4 Preparation of composite

The resin used in the present work was liquid epoxy resin with a density of 1120 kg/m<sup>3</sup>. The curing agent (hardener)

used was JOINTMINE 905-3S. The dynamic viscosities of the epoxy and hardener were 13.8 and 13.2 cp, respectively. Both the epoxy and the hardener were supplied by Covai Senu Chemicals and Polymers, Coimbatore, TamilNadu, India. During the processing of the composite, the inner surfaces of the steel mold were coated by a thin layer of polyvinyl chloride, which acted as a releasing agent for easy removal of the composite easily without any damage. The ratio of resin to hardener used was 2:1. The mixing was done by an electric stirrer. An adequate volume of CNS of 5, 10, 15, 20, 25, 30, 35 and 40% weight content was added to the resin with hardener solution and mixed thoroughly by stirrer. Compound homogeneous mixing of the filler in the resin was done by fast stirring of the stirrer, which ensures uniform mixture to avoid filler accumulation. After pouring the mixture in the mold, the closed mold was kept in a hydraulic press of about 6.5 kPa for 8 h under room temperature, which ensured complete solidification of the composites. Air bubbles were completely trapped out by hydraulic pressure. The solidified composite plate of 100 mm  $\times$  100 mm  $\times$  10 mm was removed from the mold, whose dimensions were 120  $\times$  120 mm  $\times$  12.5 mm. Post-curing was done in a hot air oven at 60°C for an hour [2]. Experiments are conducted, and the theoretical density of the composites was measured to calculate the average void content in the fabricated composites and was about 4.2  $\pm$  1.8%. It was calculated according to the ASTM D 2734 standard.

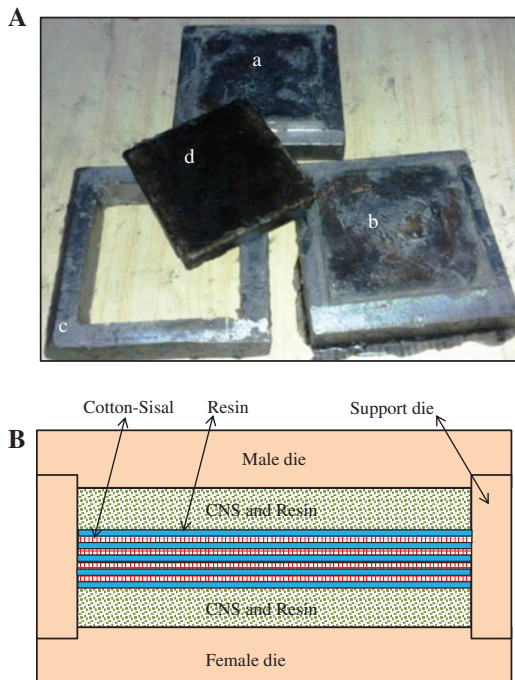


**Figure 4:** (A) Split type steel mould for composite preparation: (a) male die, (b) female die, (c) support die, and (d) composite plate; and (B) schematic diagram of the composite fabrication process.

## 3 Experimental procedure

### 3.1 Tribological experimental procedure

A POD Tribo machine (model: K93500 Koehler) was used to conduct the tribological test of the CNS-reinforced epoxy composites, as shown in Figure 5. The test was conducted as per the ASTM G99 standard. The maximum rotational speed was 2000 rpm, the diameter of the track varied from 20 mm to 140 mm, the load ranged from 10 N to 200 N, and the sliding velocity of the disk was 1.5 m/sec. The readability of the machine was 0.1 mg, and repeatability of the machine was  $\pm$ 0.1 mg. A test specimen with dimension of 8 mm (width)  $\times$  8 (depth) mm  $\times$  25 (long) mm was cut from the composite plates and fitted into the vertical specimen holder. Before the test, the counterface (ASTM B611) was polished (240 HV) using SiC abrasive paper, grade no. 1200 [3], and the specimens were polished against abrasive paper of grade no. 800 [3], which ensured proper contact between the specimen and counterface.

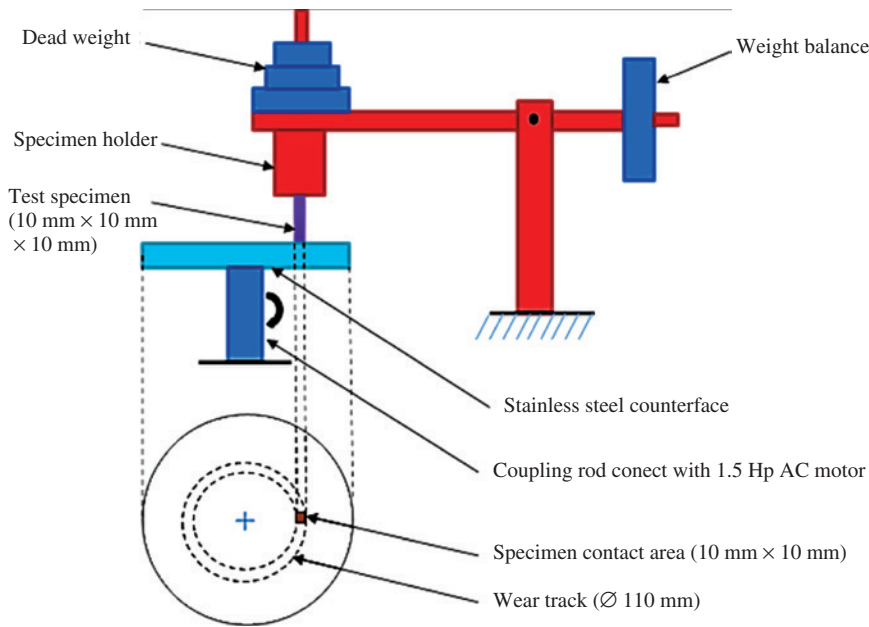


Figure 5: Schematic diagram of POD machine with test specimen.

Dry sliding abrasive wear tests were conducted under a normal applied load of 10 N, various sliding distances (0–6000 m), sliding velocity of 1.5 m/sec, and room temperature of 29°C with relative humidity of 65%–75%. The pitch circular diameter of the wear track was found to be 110 mm. The coefficient of friction ( $\mu$ ) was calculated by following relation [Eq. (1)]:

$$\text{Coefficient of friction}(\mu) = \frac{\text{measured frictional force}}{\text{normal applied load}} \quad (1)$$

The measured friction force and applied normal load were in Newton. The weight loss for each specimen was measured before and after the wear test using a 0.1-mg digital weight indicator (model: DOLPHIN DT-300). The specific wear rate ( $W_s$ ) was calculated using the following relation [Eq. (2)]:

$$\text{Specific wear rate}(W_s) = \frac{W_i - W_f}{\rho \times F_N \times D} \quad (2)$$

where  $W_s$  = specific wear rate ( $\text{mm}^3/\text{N}\cdot\text{m}$ );  $W_i$  = initial weight of the specimen (kg);  $W_f$  = final weight of the specimen (kg);  $\rho$  = density of the composite ( $\text{kg}/\text{mm}^3$ );  $F_N$  = normal applied load (N); and  $D$  = sliding distance of the specimen (m). Four identical specimens were tested for each composite (sample 1 [S1], sample 2 [S2], sample 3 [S3], and sample 4 [S4]), and the average of the four sample values (AV) was reported with a standard deviation of  $4.5 \pm 1.5\%$ . The density figures of the composites were 1.245, 1.237, 1.231, 1.225, 1.218, 1.213, 1.206 and 1.200

g/cc for 5%, 10%, 15%, 20%, 25%, 30%, 35%, and 40% weight fractions, respectively, and the average hardness values of the composites were 9.4, 9.7, 10.3, 11.1, 11.4, 11.8, 11.5, and 11.3 HV for the respective weight contents of the composite.

### 3.2 Scanning electron microscope

The microstructures of the worn-out composite pins were analyzed using the cross-section analysis method through the use of SEM (model: JEOL JSM-6390, Tamil Nadu Agricultural University, India). The scanning of the images was done with the following specification use for resolution (3.0 nm [Acc V 20 kV, WD was more than 5–15 mm and SEI], magnification of  $5 \times [\text{WD} 48 \text{ mm or less}]$ , and electron gun [accelerating voltage: 0.5–30 kV and filament: pre-centered tungsten hairpin filament]). These observations were made under room temperature of  $29 \pm 5^\circ\text{C}$  and humidity of 70%.

## 4 Results and discussion

### 4.1 Wear characteristics

The wear performance of CNS-filler-reinforced epoxy composites as a function of specific wear rates ( $W_s$ ) versus various CNS filler weight contents with constant sliding

**Table 1:** Specific wear rates of the raw CNS filler epoxy composites with various filler contents.

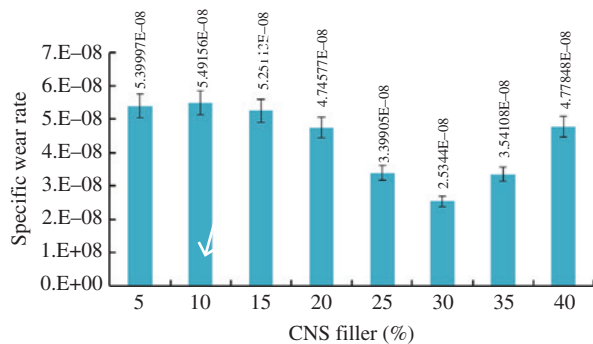
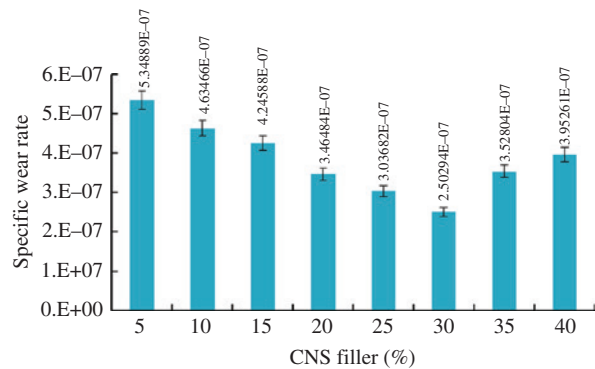
Filler contents (%)	Samples			
	S1	S2	S3	S4
5	5.10997E-08	5.52997E-08	5.62997E-08	5.32997E-08
10	5.15406E-08	5.45406E-08	5.62406E-08	5.73406E-08
15	5.13113E-08	5.35113E-08	5.51113E-08	5.01113E-08
20	4.94716E-08	4.55716E-08	4.78716E-08	4.69160E-08
25	3.56905E-08	3.35905E-08	3.23905E-08	3.42905E-08
30	2.91379E-08	2.13793E-08	2.44793E-08	2.63793E-08
35	3.19608E-08	3.29608E-08	3.39608E-08	3.47608E-08
40	4.75348E-08	4.75348E-08	4.95348E-08	4.65348E-08

velocity of 1.5 m/s and applied load of 10 N is presented in Tables 1 and 2. The wear experiments were performed with raw and NaOH-treated CNS filler composites. Four samples (S1, S2, S3, and S4) in all were taken for the wear experiments and the average values were reported for each CNS weight content, as shown in Figures 6 and 7.

The composite pin was kept on the hard surface of stainless-steel counterface for measuring the adhesive wear rate for 0–6 km. Table 1 shows  $W_s$  as quite sensitive to

**Table 2:** Specific wear rates of the NaOH-treated CNS filler epoxy composites with various filler contents.

Filler contents (%)	Samples			
	S1	S2	S3	S4
5	5.14E-07	5.45E-07	5.68E-07	5.12E-07
10	4.86E-07	4.66E-07	4.86E-07	4.16E-07
15	4.42E-07	4.26E-07	4.20E-07	4.12E-07
20	3.56E-07	3.66E-07	3.38E-07	3.26E-07
25	2.86E-07	3.26E-07	3.08E-07	2.95E-07
30	2.75E-07	2.45E-07	2.45E-07	2.35E-07
35	3.48E-07	3.69E-07	3.26E-07	3.69E-07
40	4.01E-07	4.01E-07	3.88E-07	3.93E-07

**Figure 6:** Specific wear rates of the untreated CNS filler epoxy composites with various filler contents.**Figure 7:** Specific wear rates of the treated CNS filler epoxy composites with various filler contents.

the different CNS weight contents. Generally, the increasing CNS weight content affected the wear performance of the composite.

Table 1 shows the  $W_s$  of 5, 10, and 15% raw CNS filler composites as high for four samples, and the average value was high compared to other CNS-containing composites as shown in Figure 6. This may be due to the low content of raw fillers, which tended to provide less interfacial adhesion between the filler-resinous regions. During the experiments, the resin surface area had more contact with rotating counterface instead of CNS filler contact. The material removal rate was observed to be more in resinous region rather than in the filler regions due to low surface hardness. In the four samples, the results of  $W_s$  seemed to vary highly between the samples. This may be due to the wearing out of uneven surface at the beginning of the test and smaller content of fillers. The continuous contacts of soft (composite pin) and hard (counterface) surfaces were associated to generation of wear debris (i.e. epoxy resin), which tended to form a strong back film on the wear surface, sliding between the molecular layers that might have been due to high thermo-mechanical loading between the faces. This loading generated a higher

interfacial temperature that led to more epoxy debris. This temperature softened the epoxy region, which produced the back film and higher material removal. The film formation by wear debris may have been caused by the wear of resin or filler or a combination of both. Also, an enough quantity of filler was not taken for composite preparation, which led to a reduction in the real contact area (i.e. filler and resin contact together on the counterface).

In Table 1, the  $W_s$  values of 15, 20, and 25% of CNS filler composites are found to gradually decrease for the four samples compared to low filler-containing composites, while Figure 6 shows the gradual decreasing trend observed with the standard deviation. This could be due to the increasing real contact area and adequate fillers in the composites. The large volume of filler in the composites played an important role in the material removal process, and then the fillers initiated the wear. The presence of matrix regions during wearing out was gradually reduced by increasing the filler content and surface hardness values, which would lower thermo-mechanical loading. At 30% of CNS filler,  $W_s$  was found to be low compared to 25 and 35% of CNS filler containing composites and other composites. The required quantity of CNS fillers was reinforced in the composites by homogeneous mixing of the filler in the resin with the help of a mechanical mixer. The entire volume of the epoxy resin was wet with the fillers to ensure uniform distribution of the filler in the composites. The wear occurred on both the fillers and the resinous region. Figure 6 shows the gradual decreasing trend of  $W_s$  with the addition of the CNS in epoxy composite up to 30% of CNS weight content and thereafter the increases in  $W_s$  with the addition of CNS filler content. This could be due to contact conditions between the fillers with epoxy and the counter surface. During experiments, both fillers and resinous regions were worn out at maximum weight content of CNS filler composites, while the fillers experienced low shear resistance at the counterface rubbing zone, which resulted in bringing down the material removal. Then the sliding force acted on both the fillers and resinous region, which reduced the  $W_s$ . The wear debris occurred for both the fillers and resinous region and the back film formation was found to be low with the spill out of epoxy region along with fillers. This reduced the thermo-mechanical loading and higher hardness, thereby increasing the wear resistance in the composites. The trend of  $W_s$  for the four sample values was found to be almost equal. This was due to the uniform distribution of fillers in the resinous region. Despite the composites having 35% and 40% of filler content, they did not have a low wear rate. This could be due to the wearing out of more fillers at the rubbing interface. Also, the inadequate

real contact area between the fillers and resinous region had more filler tear out from the composites in the rubbing zone during the experiments.

Figure 7 shows the wear performance of the treated CNS filler composites with the effect of various filler weight contents. A similar trend was observed from the raw CNS filler composites. In Table 2, the  $W_s$  values of 5% treated CNS filler composites were found to be high for the four samples and the wear rate was found to be the same as for the raw CNS filler composites. With a further increase in the filler content,  $W_s$  was gradually reduced up to 30% of treated CNS filler containing composites. This was the consequence of the incorporation of treated filler in the composite, which increased the adhesion between the fillers and resinous region. At 30% of treated CNS, the  $W_s$  values were found to be lower for the four samples and the wear rate was around  $2.5 \times 10^{-7} \text{ mm}^3/\text{N}\cdot\text{m}$ . Simultaneous wearing out of both filler and the resinous region was a matter of fact. This wearing out was reason to be low compared to raw filler composite, which caused a lower material removal process. There are two regions for lowering the worn-out. First, the higher interfacial adhesion between the fillers and resinous region resisted the filler pull-outs during experiments. Second, the treated filler in the rubbing surfaces reduced the softening of resinous region and reduced the forming of back film by temperature. Furthermore, increasing the treated CNS filler content was found to result in low wear performance as a result of inadequate real contact area and low hardness value. At 35 and 40% of treated CNS filler,  $W_s$  values were lower compared to untreated CNS filler composites with various filler weight contents.

Figure 8 shows  $W_s$  versus sliding distance of treated CNS at 30% weight content at 10 N applied load and 1.5 m/sec sliding velocity. Increasing the sliding distance of the composite pin results in a decrease in the  $W_s$ . The wear

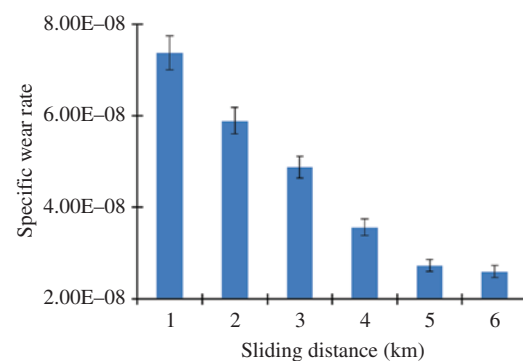


**Figure 8:** Specific wear rates of treated CNS filler composites (30%) with sliding distance.

rate was higher at low sliding distance. But increasing the sliding distance of treated CNS fillers composites was resisting the wear rate that lower the rate of wear. The trend in wear rate of the specimen for each 1 km was suddenly decreased up to 4 km. The wear rate becomes stable thereafter for the remaining 2 km. This was due to the real contact of both the filler and the resinous region on the rubbing zone. Application of normal load, sliding velocity, and filler content was subjected to resistance of the wear rate. Similarly, the  $W_s$  of betelnut polyester composite was higher at 1-km sliding distance. For every 1-km sliding distance, the  $W_s$  was low up to 6 km [17]. The sliding distance was more than 5 km; the  $W_s$  could not change, which resulted in low material removal process. Initially, a large resinous region was worn out during the experiments. This led to a higher wear rate. With a further increase in the sliding distance, the fillers and resinous region were worn out. This led to resistance of the wear. This is the main region where the wear rate was low with increasing sliding distance.

## 4.2 Friction characteristics

The friction performance of CNS-filler-reinforced epoxy composites is presented as a function of various filler contents, constant sliding velocity, and applied normal load in Tables 3 and 4. Table 3 shows the friction coefficients of raw CNS filler composites for five tested samples. The filler weight content seems to have played an important role in the friction coefficients, with good improvement in friction coefficients by the addition of raw filler in the epoxy composite. Basically, the trend of friction coefficients in 5% to 20% raw CNS filler composites was a gradual decrease for four samples. The average friction coefficients with standard deviation are plotted in Figure 9. At 5% of CNS, the

**Table 3:** Friction coefficients of the raw CNS filler epoxy composites with various filler contents.

Filler contents (%)	Samples			
	S1	S2	S3	S4
5	0.38	0.395	0.37	0.36
10	0.34	0.35	0.335	0.33
15	0.22	0.21	0.23	0.20
20	0.18	0.20	0.21	0.19
25	0.11	0.12	0.13	0.125
30	0.10	0.085	0.12	0.095
35	0.24	0.19	0.26	0.248
40	0.25	0.29	0.235	0.271

**Table 4:** Friction coefficients of the NaOH-treated CNS filler epoxy composites with various filler contents.

Filler contents (%)	Samples			
	S1	S2	S3	S4
5	0.32	0.33	0.34	0.45
10	0.30	0.34	0.32	0.33
15	0.26	0.27	0.26	0.25
20	0.19	0.15	0.165	0.175
25	0.10	0.08	0.10	0.095
30	0.06	0.08	0.09	0.075
35	0.15	0.16	0.137	0.15
40	0.28	0.26	0.245	0.27

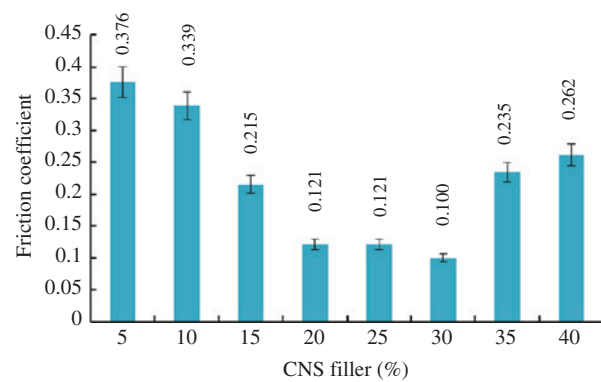


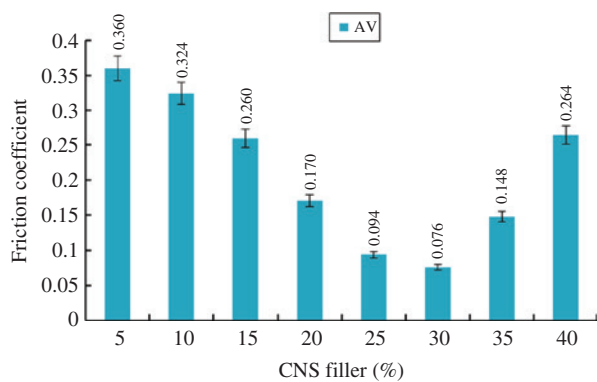
**Figure 9:** Friction coefficients of the raw CNS filler epoxy composites with various filler contents.

frictional force between the interfaces occurred in the resinous region than in the fillers in the test specimen. This could be the maximum material removal of the resinous region and a lower wear resistance. Fine particles came out from the specimen during the experiments; this might form a back film on the counterface, and this produced three different contact mechanisms. These were “cold welding,” “rupture,” and “galling” or “scoring” [1]. More epoxy fine particles ruptured from the specimens having a higher friction coefficient. At 10 to 20% of CNS, there was a gradual decrease in the friction coefficient. This effect may be a gradual increase in filler content in composites and also an increase in the real contact area. However, the fillers played an important role in the wear mechanism for the gradual reduction in the formation of back film. The coefficient of frictions from 20% to 25% CNS filler composites were the same. At 30% of CNS, the friction coefficient was found to be low due to the frictional force taken by both fillers and resinous region. These regions were ruptured to produce the fine particles (wear debris), and these filler particles were pulled out from the interfaces to avoid the formation of a back film. This could be low

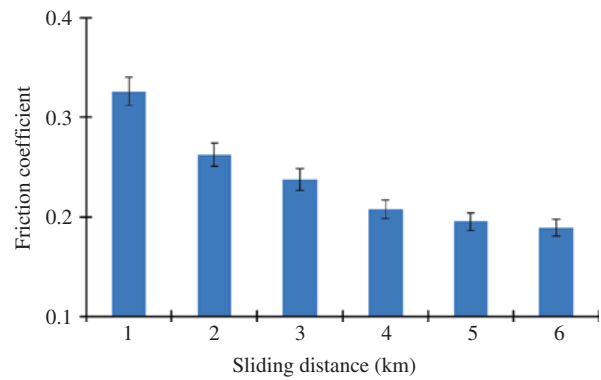
frictional coefficient. At 35%–40% of CNS, the friction coefficients were increased suddenly. This may be the frictional forces acting on the fillers rather than the resinous region. It leads to maximum material removal.

Table 3 shows the friction coefficients of treated CNS filler composites for five tested samples. These results seemed similar to those of raw CNS. Overall, the friction coefficient of treated CNS was lower than that of the raw CNS composites. This could be attributed to a higher interfacial bonding strength between the fillers and the matrix [11, 13]. The bonding strength is acting against the friction force, is lowering the volume of material removal, and is increasing the wear resistance. Figure 10 shows a gradual decrease in the friction coefficients from 5% to 25% addition of CNS filler in the composites. The friction coefficients were the same in composites containing 25% and 30% CNS filler. Here, the filler and resin were wearing out simultaneously as a result of lower wear rate. At 30% of CNS, the friction coefficient was found to be low as a result of interfacial bonding. At 35 or 40% of CNS, an increasing trend was observed by more filler incorporated in the composites. The fillers were accumulated in the matrix. This reduced the bonding strength between the filler and matrix. With higher filler content, the shear force was higher at the interface, which led to more filler coming out from the composite. The percentage difference of wear rate of the composites between CNS filler weight contents was 10% at 5% to 10% of CNS, 19.7% at 10% to 15% of CNS, 34% at 15% to 20% of CNS, 44% at 20% to 25% of CNS, 19% at 25% to 30% of CNS, 48.6% at 30% to 35% of CNS and 43.9% at 35% to 40% of CNS.

Figure 11 shows the effect of sliding distance on the friction coefficient of 30% treated CNS filler epoxy composite. The four samples were tested and the results are reported for each 1-km sliding distance. A gradual decreasing trend was found with increasing sliding distance. This



**Figure 10:** Friction coefficients of the treated CNS filler epoxy composites with various filler contents.



**Figure 11:** Friction coefficients of treated fine CNS filler composites (30%) with sliding distance.

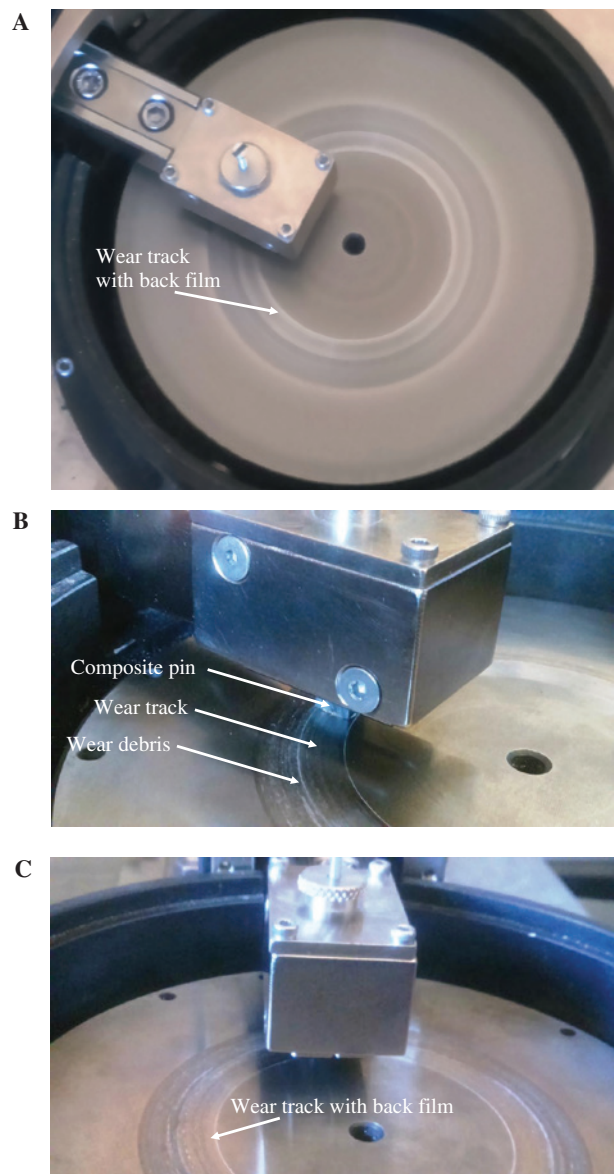


**Figure 12:** Photo image of the Back film formation on the pin-on-disk: (A) 5% of CNS, (B) 30% of CNS, and (C) 35% of CNS.

friction coefficient was found to be smaller compared to untreated CNS filler composites. The friction coefficients of each sample for all sliding distances were found to have less deviation by a better interfacial adhesion between the filler and matrix.

### 4.3 Examination of the counterface and CNS worn surfaces' morphology

Photo images of the counterface and worn surfaces' morphology of specimens in the worn surface with a constant sliding velocity of 1.5 m/sec and applied normal load of 10 N are presented in Figures 12 and 13. The continuous wearing out of the composite forms a thin layer of back film between the specimen and counterface, which affected the wear performance. The bonding strength between the filler or the natural fibers on the polymer was found to be satisfactory for various mechanical properties [2, 10].

A closer visual examination of Figures 12A and 13A shows clear evidence of the formation of a thin back film on the disk and the worn-out specimen by wear debris scattered on the entire surface. The composite containing 5% of CNS shows a large amount in resinous region, which was worn out to form the thin back film on the specimen (Figure 13A) and disk. The continuous contact of the specimen on the rotating counterface increased the interface temperature, which had a high material removal. This was the evidence of plastic deformation of resin to form

the high intimate contact and the thin back film on the counterface. It was clear that the contribution of the filler was limited on the wear mechanism; this could increase the microcutting, microplowing, and plastic deformation in the resinous region. In addition to this, the low volume of fillers in the composites increased the brittle nature of the epoxy resin and formed a microfracture on the worn surface (Figure 13A). Further, the bonding strength between the fillers and epoxy in the composites was found to be low with lower CNS content, which results in low bonding area. This reduced the wear resistance.

The composites contain 15% of CNS with a little more filler compared to above. The rate of material removal was lower than for the above composites; the filler played a significant role on the wear. The back film formation was not scattered on the entire surface of the specimen (Figure 13B), and friction coefficient was found to be low with higher friction force and shear force.

The reinforcement of 20% and 25% fillers in the composites was improved the bonding strength between the fillers and resin. This was lower the wear rate and coefficient compared to low CNS containing composites. Figure 13C and D shows the worn-out surface of the specimen; the scattered back film was seen gradually disappearing with increasing filler content. This may be due to the low thermo-mechanical contact between the filler and resin with the development of lower interface temperature. This temperature was found to be low due to a high filler content. The wear track on the counter face was seen

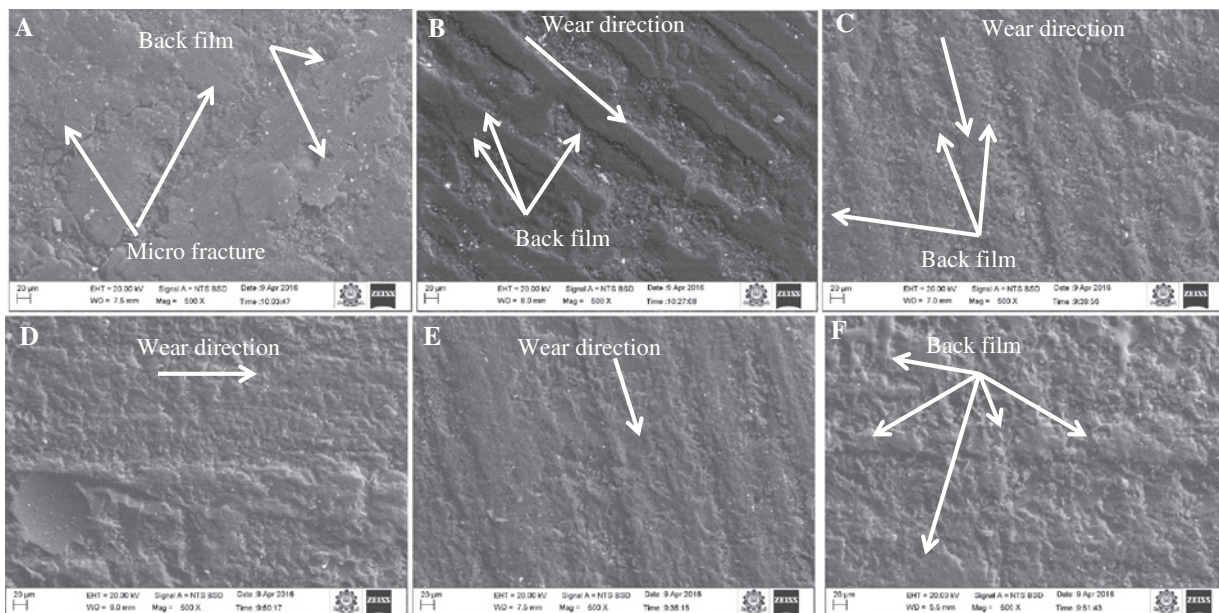


**Figure 13:** SEM image of the atrobo test worn-out surface: (A) 5% of CNS, (B) 15% of CNS, (C) 20% of CNS, (D) 25% of CNS, (E) 30% of CNS, and (F) 35% of CNS.

invisible by absence of wear debris as shown in Figure 12B. The worn surface of 30% CNS filled composites (Figure 13E) shows that the wear tract seemed linearly perpendicular to the counterface. This image shows the development of dark patches of back film on the sliding face. Disappearance of thin back film was clearly seen. Both the filler and resinous region were worn out during the experiments. This phenomenon prevented material removal from the sliding face. Also this leads to lower friction coefficient compared to result of lower CNS filler content composites. The higher bonding area with 30% filler content and 70% epoxy helps with withstanding higher interface temperature. This reduced the plastic formation of the resinous region, resulting in lower back film formation and lower shear force at the interface. This contributed to the high wear resistance of motion during the experiments and directly affected the friction coefficient and wear rate. The worn surface image of 35% of CNS content (Figure 13F) shows the back film transfer on the specimen and the nonuniform distribution of the filler in the composites. The wear track on the counterface was found to be more debris (Figure 12C). Larger volume filler was worn out during the experiments, and the matrix surface was also worn out, forming a white back film on the worn surface. This could make a slip between the friction pin and sliding counterface, leading to a high friction coefficient and or no wear on the surface. During the experiment, the counterface temperature was high and resulted in sticking of wear debris on the pin which reduces the frictional resistance.

## 5 Conclusion

CNS-filler-reinforced epoxy composites were prepared by a compression molding process with varying CNS filler weight contents. The wear behaviors evaluated by using POD machine. The following conclusions are made based on the extensive experimental work.

The friction coefficient and specific wear rate were higher at 5, 10, 15, and 20% CNS filler content containing epoxy composites. The friction coefficient and specific wear rate were low at 30% raw CNS filler content containing epoxy composites. The minimum friction coefficient was obtained in 30% of filler content due to uniform distribution of filler and wear resistance was taken by both filler and matrix. The coefficient of friction was 0.1 at 30% of CNS.

The friction coefficient and specific wear rate should decrease when treated filler content was increased up to 30% of CNS. The minimum friction coefficient was obtained in 30% of filler content as a result of better bonding and uniform distribution of the filler. The coefficient of friction ( $\mu$ ) was around 0.076 at 30% of CNS.

The morphological image showed the filler content and the back film formation on the composites. Thermo-mechanical loading occurred by the mating of CNS specimen and counterface. A higher thermo-mechanical loading occurred in the lower filler and higher filler content. This formed a back film on the specimen or the counterface. This was overcome by adding 30% CNS filler content in the epoxy composites. The CNS filler with 30% weight content has better wear properties in untreated and treated conditions. Also, the composites with lower and higher percentage of CNS filler were found higher specific wear rate. Then lower specific wear rate occurs for composites containing 30% CNS filler. Hence, the 30% of CNS in the composites obtained better wear and friction performance in treated and untreated conditions of filler.

## References

- [1] Nirmal U, Hashim J, Ahmad MMHM. *Tribol. Int.* 2015, 83, 77–104.
- [2] Sathishkumar TP, Navaneethakrishnan P, Shankar S, Rajasekar R. *Reinf. Plast. Comp.* 2013, 32, 1446–1465.
- [3] Nirmal U, Hashim J, Low KO. *Tribol. Int.* 2012, 7, 122–133.
- [4] El-Tayeb NSM. *Wear* 2009, 266, 220–232.
- [5] El-Tayeb NSM. *J. Mater. Process. Tech.* 2008, 20, 305–314.
- [6] El-Tayeb NSM. *Wear* 2008, 265, 223–235.
- [7] Aigbodion VS, Hassan SB, Agunsoye JO. *Mater. Des.* 2012, 33, 322–327.
- [8] China CW, Yousif BF. *Wear* 2009, 267, 1550–1557.
- [9] Yousif BF, Lau STW, McWilliam S. *Tribol. Int.* 2010, 43, 503–511.
- [10] Yousif BF, Nirmal U, Wong KJ. *Mater. Des.* 2010, 31, 4514–4521.
- [11] Dwivedi UK, Chand N. *J. Mater. Process. Tech.* 2009, 209, 5371–5375.
- [12] Dwivedi UK, Chand N. *Appl. Compos. Mater.* 2009, 16, 93–100.
- [13] Chand N, Dwivedi UK. *Wear* 2006, 261, 1057–1063.
- [14] Goriparthi BK, Suman KNS, Rao NM. *Compos. Part A* 2012, 43, 1800–1808.
- [15] Bajpain PK, Singh I, Madaan J. *Wear* 2013, 297, 829–840.
- [16] Ibrahim RA. *Tribol. Int.* 2015, 90, 463–466.
- [17] Lee PW, Filip P. *Wear* 2013, 302, 1404–1413.
- [18] Matejka V, Fu Z, Kukutschova J, Qi S, Jiang S, Zhang X, Yun R, Vaculik M, Heliova M, Lu Y. *Mater. Des.* 2013, 51, 847–853.
- [19] Abdel-Rahim YM, Darwish SM. *Tribol. Int.* 2010, 43, 838–843.